Article:
Thomas, SA, Mishra, B and Myneni, SCB (2020) Cellular Mercury Coordination Environment, and Not Cell Surface Ligands, Influence Bacterial Methylmercury Production. Environmental Science & Technology, 54 (7). pp. 3960-3968. ISSN 0013-936X

https://doi.org/10.1021/acs.est.9b05915

Cellular mercury coordination environment, and not cell surface ligands, influence bacterial methylmercury production

Sara A. Thomas,*[1] Bhoopesh Mishra,[2] and Satish C. B. Myneni[1]

[1] Department of Geosciences, Princeton University, Guyot Hall, Princeton, NJ, 08544

[2] School of Chemical and Process Engineering, University of Leeds, Leeds LS2 9JT, UK

* Corresponding author:

Sara A. Thomas

Email: st18@princeton.edu

Phone: (609)-258-2339

Abstract

Conversion of inorganic mercury (Hg(II)) to methylmercury (MeHg) is central to the understanding of Hg toxicity in the environment. Hg methylation occurs in the cytosol of certain obligate anaerobic bacteria and archaea possessing the *hgcAB* gene cluster. However, the processes involved in Hg(II) biouptake and methylation are not well understood. Here we examined the role of cell surface thiols, cellular ligands with the highest affinity for Hg(II) that are located at the interface between the outer membrane and external medium, on the sorption and methylation of Hg(II) by *Geobacter sulfurreducens*. The effect of added cysteine (Cys), which is known to greatly enhance Hg(II) biouptake and methylation, was also explored. By quantitatively blocking surface thiols with a thiol binding ligand (qBBr), we show that surface thiols have no significant effect on Hg(II) methylation, regardless of Cys addition. The results also identify a significant amount of cell-associated Hg-S_3/S_4 species, as studied by high energy-resolution X-ray absorption near edge structure (HR-XANES) spectroscopy, under conditions of high MeHg production (with Cys addition). In contrast, Hg-S_2 are the predominant species during low MeHg production. Hg-S_3/S_4 species may be related to enhanced Hg(II) biouptake or the ability of Hg(II) to become methylated by HgcAB and should be further explored in this context.

Introduction

Mercury (Hg) is a global pollutant that is highly bioaccumulative and neurotoxic in its chief environmental organic form (i.e., methylmercury – MeHg or CH_3Hg^+). Certain obligative anaerobic bacteria and archaea are the primary source of MeHg,[1-3] which is produced from inorganic Hg(II) in the cell cytosol.[4] Thus, understanding the biogeochemical factors that lead to the microbial biouptake and subsequent methylation of Hg(II) is crucial to develop models for determining the potential for MeHg production in the environment.

Chemical Hg(II) speciation is a critical factor that controls whether Hg(II) biouptake and methylation can occur in the environment. Hg(II) has a high affinity for reduced sulfur (i.e., thiols and sulfides), and the formation constants of Hg(II)-thiol and inorganic Hg(II)-sulfide species can be at least 20 orders of magnitude greater than those of Hg(II) complexes with carboxyls, amines, and most inorganic ligands.[5, 6] Thus in natural environments, Hg(II) is expected to be bound to thiols (e.g., natural organic matter and low molecular weight – LMW – organic ligands) and/or inorganic sulfides (e.g., particulate and dissolved mono- and polysulfides) under sulfidic conditions.[7]

While much attention has been given to understanding the biouptake of Hg(II)-thiol and Hg(II)-sulfide species by Hg-methylating organisms, the mechanisms and pathway(s) of Hg(II) biouptake are not well understood. Most studies rely on thermodynamic stability constants to obtain chemical Hg(II) speciation information for Hg(II) uptake and methylation assays.[8-15] This methodology has led to current Hg(II) biouptake paradigms, which include the passive uptake of neutral Hg(II)-sulfide complexes (e.g., HgS^0 or $Hg(HS)_2^0$)[8-11] and the active uptake of Hg(II) complexes with LMW thiols (e.g., $Hg(cysteine)_2$).[12, 13] However, microbes can alter extracellular Hg(II) speciation by the degradation or secretion of Hg(II)-binding ligands (e.g., sulfide and

cysteine)[16-20] as well as cell-associated Hg(II) speciation via reactions with cellular S-containing ligands.[16-18, 21-24] Therefore, predictions for Hg(II) speciation based on the initial composition of the exposure medium are not always accurate throughout the duration of the assay. In contrast, directly tracking the cell-associated Hg(II) coordination environment during Hg exposure assays can provide insight into the Hg(II) uptake and methylation mechanisms. Yet, only a few studies have captured Hg(II) coordination information during microbial Hg uptake[16-18, 22, 25] and even fewer have studied Hg(II) coordination in organisms actively methylating Hg[17, 25] due to the inherently low concentrations of cell-associated Hg. Furthermore, the Hg coordination environment in Hg-methylating organisms at environmentally-relevant Hg concentrations has yet to be explored.

The recent developments in high energy-resolution X-ray absorption near edge structure (HR-XANES) spectroscopy now makes the assessment of Hg(II) coordination in dilute systems (sub-ppm Hg) possible,[16, 26-30] specifically at the ambient Hg to cell ratios at which environmental Hg methylation is of concern. Herein, we employ Hg L_3-edge HR-XANES spectroscopy to directly monitor the coordination chemistry of Hg in actively Hg-methylating cells. Specifically, we explore the effect of extracellular cysteine (Cys) addition as well as the role of cell surface thiols on the sorption, methylation, and Hg(II) coordination by the model Hg-methylating bacterium *Geobacter sulfurreducens*. Cell surface thiols make up roughly 5 – 10% of the total surface functional groups,[31] can form complexes with Hg,[21-24, 31, 32] and may even adsorb or act as a nucleation site for $HgS_{(s)}$ nanoparticles.[17] Metal sorption to cell surface functional groups is a primary step in general metal biouptake models,[33] and Hg(II) sorption to surface thiols has recently been proposed to control Hg(II) uptake and methylation under environmental conditions.[20] Yet, the role of cell surface thiols in MeHg production has not been directly explored. Because

exogenous cysteine (Cys) is known to greatly enhance Hg(II) uptake and methylation by *G. sulfurreducens*,[14] we compare our results in the presence and absence of added Cys.

Materials and Methods

Bacterial strain and growth medium. *Geobacter sulfurreducens* PCA was gratefully obtained from Dr. Jeffra Schaefer, Rutgers University. *G. sulfurreducens* was grown statically at 29 ºC in a dark water bath in defined medium from Schaefer et al.[14] containing (g per L): MOPS buffer (2.1), NH_4Cl (0.005), NaH_2PO_4 (0.006), sodium acetate (0.82), sodium fumarate (6.4), resazurin (0.001), and trace metals (10 mL per L; Table S1) at pH 6.8 (adjusted with NaOH). The growth and assay media were made anoxic by boiling and cooling while bubbling with N_2 gas. Hungate tubes and acid-washed serum bottles containing the anoxic media were crimp sealed with rubber septa and autoclaved. Once exponential growth phase was reached (OD_{600} = 0.1 – 0.2), cells were washed once in the assay medium containing 10 mM MOPS buffer, 0.1 mM NH4Cl, 1.3 mM KCl, 1 mM Na-β-glycerophosphate, 0.12 mM $MgSO_4$, 1 mM sodium acetate, and 1 μg/mL resazurin at pH 6.8. Sodium fumarate was added to the assay medium after autoclaving to a final concentration of 1 mM from a filter-sterilized stock solution.

***Cell surface thiol quantification*.** The thiol concentration at the cell surface of exponentially grown *G. sulfurreducens* was quantified after reaction with (qBBr) by fluorescence spectroscopy on a Photon Technology International (PTI) Quantamaster fluorometer as described in Joe-Wong et al.[34] Cells that were washed with the assay medium were diluted to an OD_{600} of 0.015 – 0.04 in the assay medium, and 7 – 8 mL of cell suspension were distributed among 15 mL N_2-flushed, acid-washed serum vials. Microliter volumes of a qBBr stock solution that was prepared in anoxic Milli-Q were added to cell suspensions (8 mL final volume) under N_2 atmosphere and crimp sealed with butyl rubber septa. Cell suspensions were mixed with qBBr for 2 hours and those that did not

remain anoxic throughout the experiment (shown by the resazurin indicator) were not analyzed. A 2 mL aliquot was extracted with a syringe and quickly dispensed into a polystyrene fluorometer cuvette (Fisher Scientific). A fluorescence spectrum was immediately measured from 400 to 500 nm (380 nm excitation), and the fluorescence at 470 nm was selected for analysis. While only 1 scan is necessary per sample, the fluorescence measurement is stable in air up to 4 scans of ~1.5 min duration.

***Hg(II) exposure assays*.** For Hg(II) sorption/methylation experiments, 7.2 mL of cell suspension in assay medium were transferred to N_2-flushed, acid-washed 15 mL borosilicate glass serum vials under a stream of N_2 gas in the headspace. To achieve final Hg(II) concentrations of 0 – 200 nM, 0.8 mL of 10 times concentrated Hg(II) stock solution prepared in anoxic Milli-Q water was added to the cell suspension so that the final volume was 8 mL. After Hg(II) addition, vials were crimp sealed with rubber septa. A 10 mM $Hg(NO_3)_2$ stock solution in 1% HNO_3 (trace metal grade) was used for all exposure assays and stored at 4 ºC. For HR-XANES samples, the above procedure was replicated, but the final volume of cell suspension with Hg(II) addition was 50 mL in 100 mL acid-washed serum bottles. All assays involving Hg(II) were mixed for 2 hours at 150 rpm in the dark at room temperature. Vials that did not remain anoxic during the exposure assays (as determined by the resazurin indicator) were not analyzed. When the effect of qBBr was tested (i.e., blocking cell surface thiols), a microliter volume of qBBr stock solution prepared in anoxic Milli-Q was added to the cell suspension and allowed to mix for 2 hours prior to Hg addition. When the effect of Cys was tested, a microliter volume of Cys stock prepared directly before use was pre-equilibrated with Hg(II) in anoxic Milli-Q for 1 hour at 10 times the final desired concentration. The pre-equilibrated Hg(II)-Cys solution was then diluted by a factor of 10 upon addition to cell suspensions.

Total and methyl-Hg measurements. Aliquots (700 µL) for total and dissolved Hg(II) and MeHg were collected by syringe after the 2 hour mixing period with Hg (± qBBr/Cys), preserved in ~0.5% HCl in amber borosilicate glass vials and placed in the freezer until analysis. At least 3 replicates from independent experiments were measured for each sample. Total Hg measurements were made on a Lumex RA-915M Mercury Analyzer with Pyrolyzer PYRO-915+ (Solon, OH).[35] Between 50 to 200 µL of liquid sample was pipetted onto ~100 mg of activated carbon in the quartz sample boat, which was placed into the thermal decomposition chamber reaching a temperature of ~800 °C. The Hg in the sample was atomized and brought to the analysis cell by a steady air flow. The total Hg concentration was obtained by atomic absorption spectroscopy at 254 nm with Zeeman correction for background absorption. The recovery was within 100 ± 5% for a 50 nM control solution made in the assay medium. For MeHg analysis, samples were distilled by a Tekran 2750 gas manifold and heating system and analyzed by cold vapor atomic fluorescence spectroscopy (CVAFS) with a Tekran 2700 Methylmercury Analysis System as described in US EPA Method 1630. All MeHg controls and references for calibration were prepared from a Brooks Rand 1 ppm MeHg stock solution. Blanks in the assay medium (± 50 nM Hg), MeHg spiked samples, and MeHg references were run every 10 – 15 samples. In addition, controls were made in the assay medium to test recovery after distillation and derivatization. The recovery was within 100 ± 10%.

HR-XANES sample collection and measurements. The bacterial density and the initial and total recovered Hg concentration for each sample measured by HR-XANES is provided in Table S2. After mixing with Hg(II) for 2 hours (± Cys/qBBr), the cell suspension was washed twice with anoxic 0.1 M $NaClO_4$. After the final wash, the cells were resuspended in ~200 µL anoxic 0.1 M $NaClO_4$ and pipetted into a 1.5 mL microfuge tube that was fitted with an EMD Millipore

centrifugal filter unit (Mfr # UFC510024). We switched out the filter that was provided in the unit with a 0.2 μm cellulose acetate filter (Whatman) that we cut with a ~7 mm diameter hole punch. The cell suspension was centrifuged at 10,000 g for 5 minutes, collecting the cell pellet on the filter and allowing excess moisture to pass through the filter. The filter with cell pellet was sandwiched between pieces of Kapton tape, quickly plunged into LN_2, and remained frozen until analysis with HR-XANES.

The HR-XANES data were collected at the European Synchrotron Radiation Facility (ESRF) at beamline BM16 FAME-UHD. All measurements were performed in high energy resolution fluorescence detection (HERFD) mode with 5 spherically bent Si(111) crystal analyzers (bending radius = 1 m, crystal diameter = 0.1 m). The Hg $L\alpha_1$ fluorescence line was measured with a silicon drift detector (SDD, Vortex EX-90). The beam size was 100 μm × 200 μm. The monochromator was calibrated with a Se reference foil by assigning the zero value of the first derivative to the Se K-edge energy (12,658 eV), and a $HgCl_2$ powder was scanned at the start of each experiment to maintain relative energy calibration. The powder standards were finely ground, diluted to ~0.5 wt% with boron nitride, pressed into ~5 mm diameter pellets, and loaded onto a copper sample holder. The liquid reference standards were pipetted into a copper sample holder sealed on two ends with Kapton tape that was quickly plunged into LN_2 to minimize contact of the liquid with the copper as well as prevent the formation of ice. The bacterial samples were shipped to the ESRF on dry ice (< 48 hours in transit) and kept frozen during analysis. The frozen bacterial samples were quickly fixed onto copper sample holders with grease and plunged into liquid nitrogen to prevent thawing. All references and bacterial samples were measured at 10 – 15 K with some references also being measured at room temperature for comparison. The beam position on the sample was moved after every scan (duration ~35 minutes); however, no beam damage was

observed on repeat scanning locations. The data normalization was executed in Athena[36] while peak fitting was performed in Larch.[37] Details on the preparation of Hg reference standards for HR-XANES is provided in a previous publication.[16]

Results and Discussion

Quantification of cell surface thiols. The fluorophore monobromo(trimethylammonio)bimane (qBBr) binds strongly and irreversibly to thiols via nucleophilic substitution (S_N2) and has been used to estimate thiol concentration in LMW ligands and macromolecular dissolved natural organic matter.[34] qBBr is a relatively large and positively charged molecule and thus does not penetrate cell membranes (outer and cytoplasmic). It can therefore be used to quantify thiols at cell surfaces, which include thiols that are associated with the outer membrane or extracellular polymeric substance (EPS).[34, 38-41] Furthermore, a qBBr titration accurately estimates the concentrations of thiols, such as Cys and glutathione (GSH), in the assay medium from this study (Figure S1). Aliquots of *G. sulfurreducens* suspensions that were harvested in exponential growth phase were titrated with increasing concentrations of qBBr and mixed anaerobically for 2 hours, after which the fluorescence intensity at 470 nm was measured and plotted against the qBBr concentration (Figure 1). The intersection of the two best-fit lines (i.e., saturation of all accessible thiols from reactions with qBBr) from independent experiments revealed a consistent average thiol concentration at the cell surface of 55.5 ± 1.3 μmol/g bacteria (wet weight) or ~2×10^8 thiols/cell. The measurement of cell surface thiol concentration is steady up to 4 hours of mixing, and our measured value agrees well with a recent study that determined the surface thiol concentration of *G. sulfurreducens* by potentiometric titration.[22] In addition, cell suspensions titrated with qBBr remain anoxic (as determined by the resazurin indicator) for up to 4 hours, which implies that cells

retain an active metabolism to reduce the assay medium even after the blocking of surface thiols by qBBr.

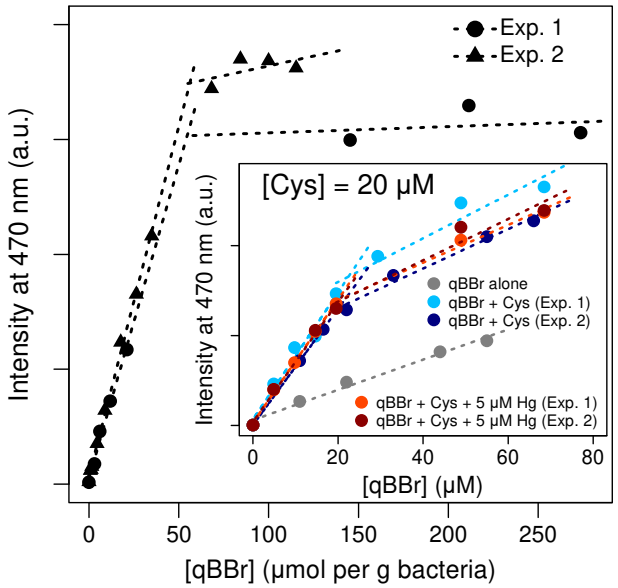

Figure 1. The fluorescence intensity of *G. sulfurreducens* cell suspension measured at 470 nm (excitation: 380 nm) as a function of the added qBBr concentration after a 2-hour exposure to estimate surface thiol density. The qBBr concentration is normalized to the cell density (g/L) for each experiment. The intersection of the two best-fit lines within each experiment indicates a cell surface thiol concentration of 56.4 and 54.6 μmol thiol per g bacteria (wet weight), respectively. Inset: qBBr titrations in the absence of bacteria of the assay medium alone (gray), with 20 μM Cys (light/dark blue), and with 20 μM Cys and then mixing with 5 μM Hg for one additional hour (light/dark red). The intersection of the two best-fit lines within each experiment estimates a Cys concentration of 20.0 ± 0.3 μM and 21.4 ± 1.6 μM with and without the addition of Hg, respectively. Thus, Hg addition does not break the qBBr-thiol bond. Thermodynamic calculations predict ~11 μM free Cys in the presence of 5 μM Hg (the remainder forming $Hg(Cys)_2$ and HgCys) in the absence of qBBr.[16]

Hg(II) binding to cell surface thiols and their impact on MeHg production. Once the thiol reacts with qBBr, the qBBr-thiol bond cannot be broken by Hg(II) addition (Figure 1 inset). Thus, qBBr can be used to selectively block cell surface thiols in Hg uptake and methylation assays. We tested how the blocking of surface thiols by qBBr as well as Cys addition affected cellular Hg(II) sorption and MeHg production after exposing cells to Hg(II) with and without Cys for 2 hours (Figure 2). The total concentration of cell surface thiols (~56 μmol per L) is approximately 1000 times greater

than the total added Hg(II) concentration for these experiments (50 nmol per L). The addition of qBBr at 1/3, 2/3 and 4/3 the concentration of the total cell surface thiols to block 1/3, 2/3 and all accessible cell surface thiols, respectively, had no effect on the sorption or methylation of 50 nM total Hg (Figure 2A,C). Regardless of the qBBr concentration added, the sorbed Hg(II) was ~90% of the total recoverable Hg(II) (Figure 2A). In addition, cells exposed to 50 nM Hg(II) only produced 1 – 2 nM total MeHg after 2 hours regardless of qBBr addition (Figure 2C). We note that the total recovered Hg (dissolved + cell-associated) does not add up to the initial added Hg after mixing both in the presence and absence of added cysteine (Figures 2A and 2B). The lower Hg recovery is likely due to Hg(II) reduction by the cytochromes of *G. sulfurreducens* and the loss of volatile Hg(0) into the headspace of the serum vial, which is known to occur under the Hg to cell ratios of this study.[42]

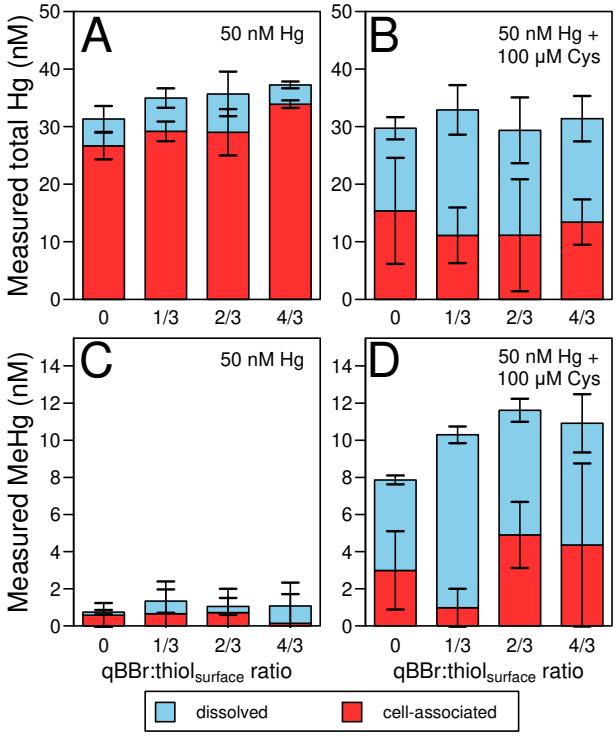

Figure 2. The dissolved and cell-associated (A,B) total Hg as well as (C,D) MeHg measured as a function of added qBBr to cell surface thiol ratio after exposure of *G. sulfurreducens* to (A,C) 50 nM Hg and (B,D) 50 nM Hg + 100 µM Cys for 2 hours. The cells were incubated with the specified qBBr concentration for 2 hours prior to Hg/Cys addition.

As expected, the addition of 100 μM Cys and 50 nM total Hg(II) to *G. sulfurreducens* drastically enhanced the total MeHg production (Figure 2D). In addition, the blocking of cell surface thiols with qBBr did not significantly affect Hg(II) sorption or methylation in the presence of added Cys (Figure 2B,D). However, the presence of Cys enhanced the fraction of dissolved Hg in the exposure medium, regardless of the fraction of surface thiols blocked by qBBr, which is likely due to a combination of efficient MeHg export from the cell[13, 14] as well as increased Hg(II) solubility (i.e., not cell-associated) due to its complexation with Cys in the exposure medium. Our findings suggest that the majority of cell surface thiols do not influence Hg(II) uptake and methylation, both in the presence and absence of added Cys. In addition, due to consistent MeHg production in the presence and absence of qBBr, these results confirm that cell physiology was minimally influenced by the inhibition of cell surface thiols. It is possible that a small fraction of surface thiols that are embedded deeper within the outer membrane (e.g. some cysteine residues of outer membrane proteins) could react with Hg but not with qBBr molecules due to size and/or steric hindrance. Therefore, the involvement of cell surface thiols in Hg methylation cannot be ruled out completely. However, blocking the majority of surface thiols from binding Hg appears to have no effect on Hg methylation. Due to the abundance of qBBr-blocked surface thiols (~ 56 μmol per L) in comparison to the total Hg concentration (50 nmol per L) in this study, bacterial surface thiols may be a large sink for Hg(II) in natural environments.

Hg(II) coordination environment in Hg-methylating bacterium. To identify the cell-associated Hg(II) species in actively Hg-methylating bacteria, we probed samples of *G. sulfurreducens* that were exposed for 2 hours to a range of Hg concentrations (50 – 200 nM) with and without cell surface thiol blocking and Cys addition using Hg L_3-edge HR-XANES spectroscopy (Figure S2). The results show that all detectable Hg(II) associated with the bacteria herein is bound to S with

the possibility of mixed Hg bonding to S and N/O in some samples (described later). The greatest variation in the cellular Hg coordination environment was found in cells exposed to Cys (Figure S2C).

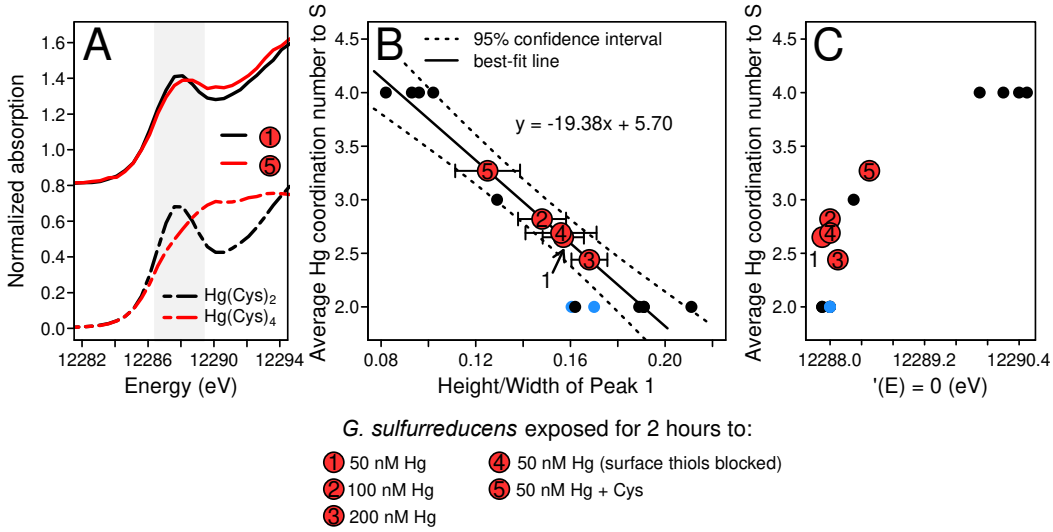

Figure 3. (A) Normalized Hg L_3-edge HR-XANES of aqueous standards of $Hg(Cys)_2$ (pH = 3) and $Hg(Cys)_4$ (pH = 11) as well as cell pellets of *G. sulfurreducens* exposed to 50 nM Hg (1) and 50 nM Hg with 100 µM Cys (5) for 2 hours. (B) The ratio of the height to the width of the deconvoluted near-edge HR-XANES Gaussian peak (Peak 1) plotted against the known average Hg coordination number to S for Hg standards from this study and from Manceau et al.[26, 44] (black dots). A description of the spectral deconvolution method is provided in the SI (Part S1). A best-fit line with 95% confidence interval was calculated from the black dots only. The blue dots represent $Hg(Cys)_2$ and $Hg(GSH)_2$ made at pH 7.5 from Bourdineaud et al., where an amine/carboxyl group is also included in the coordination sphere (i.e., $Hg[(SR)_2 + (N/O)_{1\text{-}2}]$).[27] The red circles represent sample spectra of *G. sulfurreducens* exposed to 50 nM Hg, 100 nM Hg, 200 nM Hg, 50 nM Hg with surface thiols quantitatively blocked by qBBr, and 50 nM Hg with 100 µM Cys for 2 hours. The error bars depict the calculated uncertainty of the height/width parameter from the fit model. (C) The average Hg coordination number to S of Hg standards and samples from subplot B plotted against the energy in the edge region at which the first derivative of the HR-XANES is equal to zero (µ'(E) = 0).

Detailed metal coordination environments in unknown samples are typically obtained by comparing their XANES spectra with those of structurally well-characterized models. A similar attempt to identify the Hg coordination environments in this study by linear combination fit is not appropriate because our library of standards does not entirely match the experimental spectra. HR-

XANES is highly sensitive to structural distortions and higher coordination shells,[43] which likely explains the dissimilarities between the spectra of dilute Hg(II) species that form in the bacteria from this study and the pure aqueous and crystalline Hg(II) standards of our library. However, the average Hg(II)-S coordination number can be estimated by examining the peak intensity and width of the lowest energy transition in Hg L_3-edge HR-XANES spectra, which corresponds to the Hg $2p_{3/2}$ to hybridized Hg 6s5d transition.[44] A sharp and intense near-edge peak is indicative of linear 2-coordinate Hg-S bonds (see $Hg(Cys)_2$ of Figure 3A).[30] Deviations from linearity caused by distortion or an additional atom in the coordination sphere (e.g., N, O, or S) produce a smaller peak amplitude.[29] Manceau et al. obtained a Hg L_3-edge HR-XANES spectrum of a trigonal $Hg(SR)_3$ complex, which has a very small near-edge peak,[44] while spectra of Hg bound to 4 S atoms in tetrahedral geometry (i.e., $Hg(SR)_4$ and β-HgS) lack a visible near-edge peak (see $Hg(Cys)_4$ of Figure 3A).[16, 28, 30, 44]

We have developed a method that involves spectral deconvolutions of Hg L_3-edge HR-XANES spectra of many compounds with Hg-S coordination to extract Hg coordination information. Specifically, we deconvoluted the spectra into 4 Gaussian peaks and an error function and further analyzed the Gaussian peak in the near-edge, hereafter referred to as Peak 1 (SI Part S1). A standard curve was created by plotting the ratio of the height to the width (2σ) of Peak 1 against the known average Hg-S coordination number using spectra from this study, Manceau et al.,[26, 44] and Boudineaud et al.[27] (Figure 3B). Because the $Hg\text{-}S_2$, $Hg\text{-}S_3$, and $Hg\text{-}S_4$ species lie in distinct regions of the standard curve in Figure 3B, this curve can estimate the average Hg(II) coordination number to S in samples that contain Hg predominantly bound to S. However, the curve is not very sensitive to mixed coordination environments of S and N/O. This is shown by comparing the height to width ratio of Peak 1 for the $Hg\text{-}S_2$ species and the two $Hg[(SR)_2 + NH_2]$

species (blue dots; Figure 3B), which lie in the same range. However, it is possible to differentiate Hg[$(SR)_2$ + $(N/O)_{1-2}$] binding from mixed Hg-S_2 and Hg-S_3/S_4 binding using the energy of Peak 1 (defined as the energy in the edge region at which the HR-XANES derivative equals zero), which is similar for Hg-S_2 and Hg[$(SR)_2$ + $(N/O)_{1-2}$] species but differs between Hg-S_2 and Hg-S_3/S_4 species (Figure 3C). We note that Hg-C bonding due to MeHg formation does not impact the interpretation of the results in this study because our MeHg analysis shows that cell-associated MeHg (likely as MeHg-Cys[29]) is < 20% of the total cell-associated Hg for the sample involving Cys and negligible (< 2%) for the other 4 samples.

Our analysis of the samples of *G. sulfurreducens* that were exposed to 50 – 200 nM total Hg indicates that the cell-associated Hg is bound to S with an average coordination number of 2 – 3 (range includes 95% confidence interval and consideration of Hg[$(SR)_2$ + $(N/O)_{1-2}$] binding; Figure 3B). This average Hg coordination number does not change when the surface thiols are quantitatively blocked by qBBr (Figure 3B). In contrast, the sample with Cys addition has a significantly larger Hg coordination number to S of 3.3 ± 0.2 (Figure 3B). This sample also has a near-edge HR-XANES peak energy that is 0.5 eV greater than the other samples (Figure 3C). This shift in energy confirms independently a larger Hg coordination number to S and provides further evidence that the sample with Cys addition is significantly different than the others. Finally, there is additional evidence for mixed Hg[$(SR)_2$ + $(N/O)_{1-2}$] coordination in the samples of *G. sulfurreducens* exposed to 100 nM Hg as well as 50 nM Hg with the surface thiols blocked due to a left-shifted edge energy above the near-edge peak (Figure S2A and S2B).[29] Mixed Hg[$(SR)_2$ + $(N/O)_{1-2}$] binding environments occur when Hg binds to LMW thiols of biological origin at neutral pH (i.e., GSH).[27] Due to the abundance of LMW thiols like GSH in bacteria,[45] Hg[$(SR)_2$ + $(N/O)_{1-2}$] binding could be a result of increased Hg binding to LMW thiols.

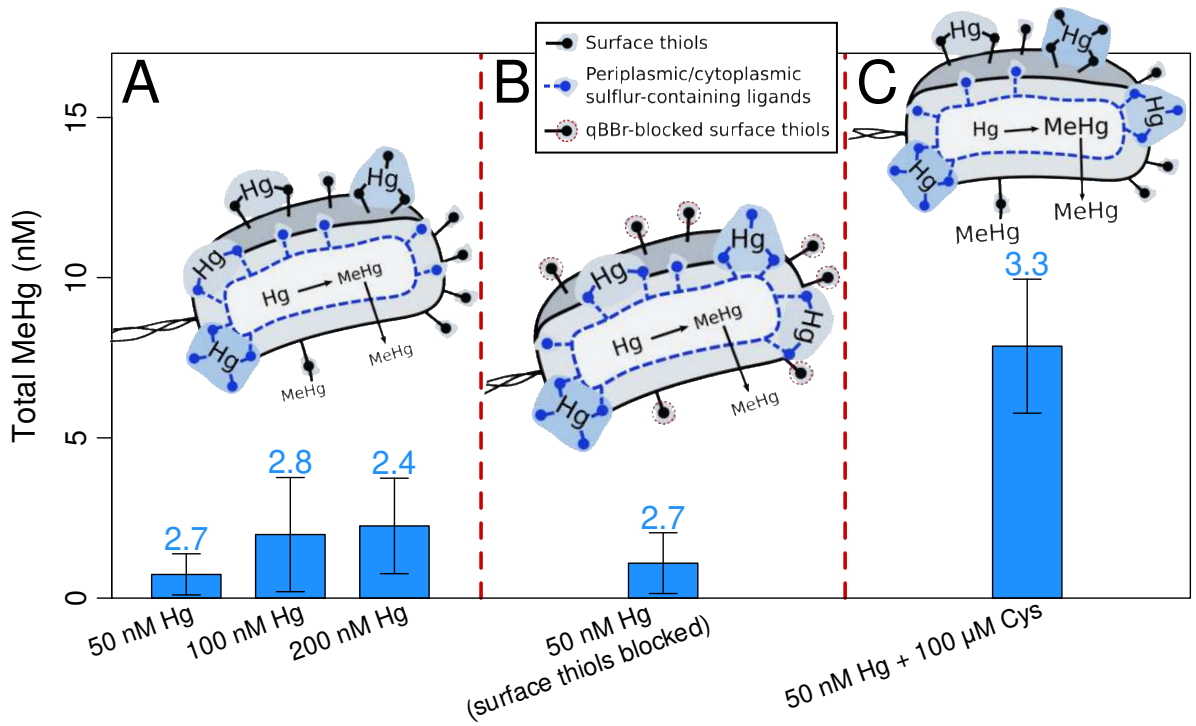

Figure 4. The total MeHg concentration (nM) produced by *G. sulfurreducens* after exposure to 50 – 200 nM total Hg for 2 hours is plotted with the average Hg coordination number to S in the cell pellet for each sample (blue numbers above bars; determined from Figure 3) to understand the relationship between cellular Hg coordination and MeHg production. We did not determine the localization of cell-associated Hg in this study; thus, the illustration merely proposes the Hg distribution among surface thiols and periplasmic/cytoplasmic S-containing ligands while satisfying the measured average cell-associated Hg coordination number to S. (A) The cell-associated Hg is coordinated on average to between 2 and 3 S atoms considering the 95% confidence interval and the possibility of mixed Hg[$(SR)_2$ + $(N/O)_{1-2}$] binding causing a slight overestimation of the Hg-S coordination number. These conditions are linked to relatively low MeHg production. (B) When surface thiols are completely blocked by qBBr, the average Hg coordination number to S is also 2 – 3 and MeHg production is unchanged. Because the surface thiols are fully blocked, Hg is likely distributed among periplasmic/cytoplasmic S-containing ligands. (C) When 50 nM Hg is added with 100 µM Cys, the cell-associated Hg is coordinated on average to 3.3 S atoms, and MeHg production is relatively high. Due to the high MeHg concentration and requirement that Hg be in the cytosol for MeHg production, Hg must be coordinated to some intracellular (periplasmic/cytoplasmic) ligands.

Implications for Hg biouptake and methylation. Our results indicate that a vast majority of cell surface thiols on a Hg-methylating organism are not involved in Hg(II) biouptake and methylation. In addition, we show that the cell-associated Hg(II)-S coordination number is positively correlated with MeHg production, as opposed to the ability of cell surface thiols to bind and retain Hg (Figure 4). When the average Hg(II) coordination number to S is low (< 3), MeHg production is also low

(Figure 4A), regardless of whether the cell surface thiols are blocked by qBBr (Figure 4B). Likewise, the addition of Hg that was pre-equilibrated with Cys led to the highest cell-associated Hg coordination number to S (3.3) and the highest MeHg production by *G. sulfurreducens* (Figure 4C). In order to satisfy an average coordination number to S of 3.3, Hg can exist either as predominantly Hg-S_3 or a mixture of Hg-S_2, Hg-S_3, and Hg-S_4 with the likely presence of Hg-S_4 in both cases to push the coordination number above 3. The correlation between Hg-S_3/S_4 species and MeHg production could be due to the species' enhanced bioavailability or connection to the form of Hg that is methylated. An indirect reason could also lead to enhanced Hg methylation, such as the formation of an intermediate complex, which is manifested by increased Hg-S coordination number. Regardless of the exact mechanism, the formation of Hg species with coordination numbers to S at or above 3 must either induce or be byproducts of the conditions favorable for MeHg production.

Cell-associated Hg-S_4 species would likely be comprised of Hg binding to inorganic sulfur (i.e., β-HgS), as opposed to organic sulfur (i.e., $Hg(SR)_4$). Inorganic Hg(II)-sulfides form readily with sulfide ions,[46, 47] can precipitate extracellularly (and potentially intracellularly) in non-dissimilatory sulfate reducing bacterial suspensions without sulfide additions,[16-18] and can even form directly from Hg(II)-thiol complexes.[30, 48] In contrast, the formation of $Hg(SR)_4$ at neutral pH is highly unfavorable.[49] It is notable that the HR-XANES do not indicate cell-associated bulk β-HgS or $Hg(SR)_4$ for any bacteria sample. However, small cell-associated Hg-S clusters with β-HgS-like local Hg coordination (i.e., analogous to Fe-S clusters), as described by Manceau et al.,[27, 50] are possible, especially due to the low Hg concentrations associated with the bacteria samples. Because Hg-S_4 is most likely present in the sample with Cys addition and *G. sulfurreducens* is known to degrade exogenous Cys into sulfide under identical exposure conditions as this study,[17]

383 the nucleation of Hg-S nanoclusters with β-HgS-like local coordination is possible, as suggested
384 previously.[16, 17] If cell-associated Hg is present as Hg-S_3, we predict the trigonal coordination of
385 Hg with 3 structurally connected thiols, which is the most stable Hg-S_3 species at physiological
386 pH[49] and has been observed in proteins (e.g., Hg-MerR in organisms with the mer operon).[51] The
387 most stable and common Hg(II)-thiol complexes in biological samples are linear, 2-coordinate.[52]
388 Therefore, the cell-associated Hg-S_2 species that we observe are likely $Hg(SR)_2$, with the
389 possibility of mixed $Hg[(SR)_2 + (N/O)_{1-2}]$ coordination.

390 Curiously, if the Hg-S_4 species is directly related to Hg methylation, it is highly unlikely
391 that this is the species that accepts a methyl group to become MeHg because the Hg coordination
392 sphere is already fully occupied with 4 S atoms. Hg methylation by HgcAB is depicted in the
393 literature as the donation of a methyl carbanion (CH_3^-) from HgcA to a $Hg(SR)_2$ complex, using
394 HgcB as an electron donor to reduce the corrinoid cofactor of HgcA.[52, 53] However, the assumption
395 that $Hg(SR)_2$ accepts a CH_3^- group is solely due to the previous understanding that $Hg(SR)_2$ is the
396 predominant form of Hg in cells.[52, 54] An interesting study would explore the possibility of the
397 methylation of Hg-S_3 or Hg-S_4 species, for example, considering a change in Hg coordination by
398 ligand exchange reactions so that the Hg coordination sphere could accept a methyl group. Site-
399 directed mutagenesis of 3 conserved Cys residues in *hgcB* revealed that at least two (i.e., Cys73
400 and Cys94 or Cys95) are required for Hg methylation,[53] and it is possible that 2 or 3 of these Cys
401 residues bind Hg while a methyl group is transferred from HgcA. A $Hg(SR)_3$ binding structure,
402 analogous to Hg-MerR, would be highly stable[51] and should outcompete Hg-S_2 species and
403 possibly even inorganic Hg-S_4 species. The coordination of Hg to 3 Cys residues of HgcB could
404 itself contribute to our observation of a possible Hg-S_3 species, although the reported abundance
405 of HgcAB in cells is very low.[55, 56]

406 The *hgcAB* gene cluster responsible for MeHg production is expressed constitutively and
407 is not responsive to Hg.[57] Therefore, Hg biouptake to the cytosol so that Hg reaches the HgcAB
408 active sites is likely the foremost cause for Hg-methylation. In light of the previous evidence
409 attributing MeHg production to the passive diffusion of neutral Hg(II)-sulfide species,[8-11] it is
410 possible that Cys leads to enhanced MeHg production due to the formation of cell-associated
411 Hg(II)-sulfide species (i.e., Hg-S_4) that can passively diffuse through the cell membrane layers.
412 The adsorption of Hg(II) to cell surface thiols has been proposed to immobilize Hg(II) against
413 biouptake.[58-60] Thus, the formation of highly stable Hg-S_4 species may enable Hg(II) to bypass
414 binding to cell surface thiols, promoting Hg(II) biouptake into the cytosol. This hypothesis
415 supports our finding that blocking cell surface thiols had no effect on Hg(II) methylation in the
416 presence of added Cys. In addition, recent evidence suggests that the biodegradation of Cys to
417 sulfide and the coexistence of these reduced sulfur species is necessary for Hg(II) uptake by
418 *Escherichia coli* exposed to excess Cys.[16] The necessity of Hg(II)-sulfide species formation for
419 biouptake in the presence of excess Cys can explain the observation that Hg(II) biouptake by *G.*
420 *sulfurreducens* is enhanced by Cys but inhibited by similar thiols that are not readily degradable
421 to sulfide (e.g., GSH and penicillamine) under otherwise identical conditions.[13] Lastly, at high Cys
422 concentrations[14] or in a mutant *G. sulfurreducens* strain that lacks outer membrane proteins
423 (Δ*omcBESTZ*),[15] Hg(II) uptake and methylation in the presence of Cys is inhibited, which could
424 be related to the inability to degrade enough Cys to enable Hg(II)-sulfide species (i.e., Hg-S_4)
425 formation.

426 This study indicates that the average cell-associated Hg coordination number to S is
427 influential to MeHg production by a model Hg-methylating bacterium while the abundance of cell
428 surface thiols capable of binding Hg(II) is not. We propose that the Hg-S_3/Hg-S_4 species, whose

formation correlates with MeHg production, are highly stable and sufficiently small Hg(II)-sulfide clusters with enhanced biouptake potential (possibly by passive diffusion). In the cytosol, the Hg-S_3/Hg-S_4 species may undergo a ligand exchange reaction, potentially with the 3 Cys residues of HgcB, prior to the addition of a methyl group to the coordination sphere to form MeHg. The link between Hg-S_3/Hg-S_4 species formation and Hg(II) biouptake as well as the methylation of highly stable Hg(II) species should be explored further. In addition, by identifying unexpected cell-associated Hg-S_3/Hg-S_4 species, we demonstrate the importance of characterizing cell-associated Hg coordination chemistry during Hg biouptake and methylation assays. Experimental approaches to directly obtain coordination information, such as HR-XANES spectroscopy, have the potential to shed light on the bioavailability of other metal species as well.

Acknowledgements

This work is supported by the National Science Foundation under grant EAR-1424899 and the Scott Vertebrate Fund of the Department of Geosciences, Princeton University. The experiments were performed on beamline BM16 – UHD-FAME – at the European Synchrotron Radiation Facility (ESRF), Grenoble, France. The FAME-UHD project is financially supported by the French "grand emprunt" EquipEx (EcoX, ANR-10-EQPX-27-01), the CEA-CNRS CRG consortium, and the INSU CNRS institute. We are grateful for the beamline assistance of Dr. Mauro Rovezzi at BM16. We also thank Dr. Jeffra Schaefer for supplying the *G. sulfurreducens* strain as well as providing helpful information on the anaerobe culture and Hg methylation assays. We appreciate the assistance of Xiaoshuai He during MeHg analysis. Finally, we thank Dr. Alain Manceau for helpful comments in reviewing this manuscript.

Supporting Information

Thiol quantification control experiments, HR-XANES spectra of bacterial samples, protocol for spectral deconvolution of HR-XANES, deconvoluted HR-XANES spectra, parameters of deconvoluted HR-XANES spectra.

References

1. Gilmour, C. C.; Bullock, A. L.; McBurney, A.; Podar, M.; Elias, D. A., Robust mercury methylation across diverse methanogenic archaea. *Mbio* **2018,** *9*, (2).

2. Podar, M.; Gilmour, C. C.; Brandt, C. C.; Soren, A.; Brown, S. D.; Crable, B. R.; Palumbo, A. V.; Somenahally, A. C.; Elias, D. A., Global prevalence and distribution of genes and microorganisms involved in mercury methylation. *Science Advances* **2015,** *1*, (9).

3. Gilmour, C. C.; Podar, M.; Bullock, A. L.; Graham, A. M.; Brown, S. D.; Somenahally, A. C.; Johs, A.; Hurt, R. A.; Bailey, K. L.; Elias, D. A., Mercury methylation by novel microorganisms from new environments. *Environmental Science & Technology* **2013,** *47*, (20), 11810-11820.

4. Parks, J. M.; Johs, A.; Podar, M.; Bridou, R.; Hurt, R. A.; Smith, S. D.; Tomanicek, S. J.; Qian, Y.; Brown, S. D.; Brandt, C. C.; Palumbo, A. V.; Smith, J. C.; Wall, J. D.; Elias, D. A.; Liang, L. Y., The genetic basis for bacterial mercury methylation. *Science* **2013,** *339*, (6125), 1332-1335.

5. Liem-Nguyen, V.; Skyllberg, U.; Björn, E., Thermodynamic modeling of the solubility and chemical speciation of mercury and methylmercury driven by organic thiols and micromolar sulfide concentrations in boreal wetland soils. *Environmental Science & Technology* **2017,** *51*, (7), 3678-3686.

6. Morel, F. M. M.; Kraepiel, A. M. L.; Amyot, M., The chemical cycle and bioaccumulation of mercury. *Annu Rev Ecol Syst* **1998,** *29*, 543-566.

7. Skyllberg, U., Competition among thiols and inorganic sulfides and polysulfides for hg and mehg in wetland soils and sediments under suboxic conditions: Illumination of controversies and implications for mehg net production. *J Geophys Res-Biogeo* **2008,** *113*.

8. Benoit, J. M.; Gilmour, C. C.; Mason, R. P., Aspects of bioavailability of mercury for methylation in pure cultures of desulfobulbus propionicus (1pr3). *Applied and Environmental Microbiology* **2001,** *67*, (1), 51-58.

9. Benoit, J. M.; Gilmour, C. C.; Mason, R. P., The influence of sulfide on solid phase mercury bioavailability for methylation by pure cultures of desulfobulbus propionicus (1pr3). *Environmental Science & Technology* **2001,** *35*, (1), 127-132.

10. Benoit, J. M.; Gilmour, C. C.; Mason, R. P.; Heyes, A., Sulfide controls on mercury speciation and bioavailability to methylating bacteria in sediment pore waters. *Environmental Science & Technology* **1999,** *33*, (6), 951–957.

11. Drott, A.; Lambertsson, L.; Björn, E.; Skyllberg, U., Importance of dissolved neutral mercury sulfides for methyl mercury production in contaminated sediments. *Environmental Science & Technology* **2007,** *41*, (7), 2270-2276.

12. Schaefer, J. K.; Szczuka, A.; Morel, F. M. M., Effect of divalent metals on hg(ii) uptake and methylation by bacteria. *Environmental Science & Technology* **2014,** *48*, (5), 3007-3013.

13. Schaefer, J. K.; Rocks, S. S.; Zheng, W.; Liang, L. Y.; Gu, B. H.; Morel, F. M. M., Active transport, substrate specificity, and methylation of hg(ii) in anaerobic bacteria. *P Natl Acad Sci USA* **2011,** *108*, (21), 8714-8719.

14. Schaefer, J. K.; Morel, F. M. M., High methylation rates of mercury bound to cysteine by geobacter sulfurreducens. *Nat Geosci* **2009,** *2*, (2), 123-126.

15. Lin, H.; Lu, X.; Liang, L. Y.; Gu, B. H., Cysteine inhibits mercury methylation by geobacter sulfurreducens pca mutant delta omcbestz. *Environ Sci Tech Let* **2015,** *2*, (5), 144-148.

16. Thomas, S. A.; Catty, P.; Hazemann, J.-L.; Michaud-Soret, I.; Gaillard, J.-F., The role of cysteine and sulfide in the interplay between microbial hg(ii) uptake and sulfur metabolism. *Metallomics* **2019,** *11*, (7), 1219-1229.

17. Thomas, S. A.; Rodby, K. E.; Roth, E. W.; Wu, J.; Gaillard, J.-F., Spectroscopic and microscopic evidence of biomediated hgs species formation from hg(ii)–cysteine complexes: Implications for hg(ii) bioavailability. *Environmental Science & Technology* **2018,** *52*, (17), 10030-10039.

18. Thomas, S. A.; Gaillard, J.-F., Cysteine addition promotes sulfide production and 4-fold hg(ii)–s coordination in actively metabolizing escherichia coli. *Environmental Science & Technology* **2017,** *51*, (8), 4642-4651.

19. Graham, A. M.; Aiken, G. R.; Gilmour, C. C., Dissolved organic matter enhances microbial mercury methylation under sulfidic conditions. *Environmental Science & Technology* **2012,** *46*, (5), 2715-2723.

20. Adediran, G. A.; Liem-Nguyen, V.; Song, Y.; Schaefer, J. K.; Skyllberg, U.; Björn, E., Microbial biosynthesis of thiol compounds: Implications for speciation, cellular uptake, and methylation of hg(ii). *Environmental Science & Technology* **2019,** *53*, (14), 8187-8196.

21. Thomas, S. A.; Tong, T. Z.; Gaillard, J. F., Hg(ii) bacterial biouptake: The role of anthropogenic and biogenic ligands present in solution and spectroscopic evidence of ligand exchange reactions at the cell surface. *Metallomics* **2014,** *6*, (12), 2213-2222.

22. Mishra, B.; Shoenfelt, E.; Yu, Q.; Yee, N.; Fein, J. B.; Myneni, S. C. B., Stoichiometry of mercury-thiol complexes on bacterial cell envelopes. *Chem Geol* **2017,** *464*, 137-146.

23. Dunham-Cheatham, S.; Mishra, B.; Myneni, S.; Fein, J. B., The effect of natural organic matter on the adsorption of mercury to bacterial cells. *Geochim Cosmochim Ac* **2015,** *150*, 1-10.

24. Dunham-Cheatham, S.; Farrell, B.; Mishra, B.; Myneni, S.; Fein, J. B., The effect of chloride on the adsorption of hg onto three bacterial species. *Chem Geol* **2014,** *373*, 106-114.

25. Colombo, M. J.; Ha, J. Y.; Reinfelder, J. R.; Barkay, T.; Yee, N., Anaerobic oxidation of hg(0) and methylmercury formation by desulfovibrio desulfuricans nd132. *Geochim Cosmochim Ac* **2013,** *112*, 166-177.

26. Manceau, A.; Bustamante, P.; Haouz, A.; Bourdineaud, J. P.; Gonzalez-Rey, M.; Lemouchi, C.; Gautier-Luneau, I.; Geertsen, V.; Barruet, E.; Rovezzi, M.; Glatzel, P.; Pin, S., Frontispiece: Mercury(ii) binding to metallothionein in mytilus edulis revealed by high energy-resolution xanes spectroscopy. *Chemistry – A European Journal* **2019,** *25*, (4), 997-1009.

27. Bourdineaud, J.-P.; Gonzalez-Rey, M.; Rovezzi, M.; Glatzel, P.; Nagy, K. L.; Manceau, A., Divalent mercury in dissolved organic matter is bioavailable to fish and accumulates as dithiolate and tetrathiolate complexes. *Environmental Science & Technology* **2019,** *53*, (9), 4880-4891.

28. Manceau, A.; Merkulova, M.; Murdzek, M.; Batanova, V.; Baran, R.; Glatzel, P.; Saikia, B. K.; Paktunc, D.; Lefticariu, L., Chemical forms of mercury in pyrite: Implications for predicting mercury releases in acid mine drainage settings. *Environmental Science & Technology* **2018,** *52*, (18), 10286-10296.

29. Manceau, A.; Enescu, M.; Simionovici, A.; Lanson, M.; Gonzalez-Rey, M.; Rovezzi, M.; Tucoulou, R.; Glatzel, P.; Nagy, K. L.; Bourdineaud, J. P., Chemical forms of mercury in human hair reveal sources of exposure. *Environmental Science & Technology* **2016,** *50*, (19), 10721-10729.

30. Manceau, A.; Lemouchi, C.; Enescu, M.; Gaillot, A. C.; Lanson, M.; Magnin, V.; Glatzel, P.; Poulin, B. A.; Ryan, J. N.; Aiken, G. R.; Gautier-Luneau, I.; Nagy, K. L., Formation of mercury sulfide from hg(ii)-thiolate complexes in natural organic matter. *Environmental Science & Technology* **2015,** *49*, (16), 9787-9796.

31. Fein, J. B.; Yu, Q.; Nam, J.; Yee, N., Bacterial cell envelope and extracellular sulfhydryl binding sites: Their roles in metal binding and bioavailability. *Chem Geol* **2019,** *521*, 28-38.

32. Mishra, B.; O'Loughlin, E. J.; Boyanov, M. I.; Kemner, K. M., Binding of hg-ii to high-affinity sites on bacteria inhibits reduction to hg-0 by mixed fe-ii/iii phases. *Environmental Science & Technology* **2011,** *45*, (22), 9597-9603.

33. Worms, I.; Simon, D. F.; Hassler, C. S.; Wilkinson, K. J., Bioavailability of trace metals to aquatic microorganisms: Importance of chemical, biological and physical processes on biouptake. *Biochimie* **2006,** *88*, (11), 1721-1731.

34. Joe-Wong, C.; Shoenfelt, E.; Hauser, E. J.; Crompton, N.; Myneni, S. C. B., Estimation of reactive thiol concentrations in dissolved organic matter and bacterial cell membranes in aquatic systems. *Environmental Science & Technology* **2012,** *46*, (18), 9854-9861.

35. Sholupov, S.; Pogarev, S.; Ryzhov, V.; Mashyanov, N.; Stroganov, A., Zeeman atomic absorption spectrometer ra-915+ for direct determination of mercury in air and complex matrix samples. *Fuel Processing Technology* **2004,** *85*, (6), 473-485.

36. Ravel, B.; Newville, M., Athena, artemis, hephaestus: Data analysis for x-ray absorption spectroscopy using ifeffit. *J Synchrotron Radiat* **2005,** *12*, 537-541.

37. Newville, M., Larch: An analysis package for xafs and related spectroscopies. *J Phys Conf Ser* **2013,** *430*.

38. Wang, Y. W.; Yu, Q.; Mishra, B.; Schaefer, J. K.; Fein, J. B.; Yee, N., Adsorption of methylmercury onto geobacter bemidijensis bem. *Environmental Science & Technology* **2018,** *52*, (20), 11564-11572.

39. Yu, Q.; Fein, J. B., Enhanced removal of dissolved hg(ii), cd(ii), and au(iii) from water by bacillus subtilis bacterial biomass containing an elevated concentration of sulfhydryl sites. *Environmental Science & Technology* **2017,** *51*, (24), 14360-14367.

40. Yu, Q.; Fein, J. B., Sulfhydryl binding sites within bacterial extracellular polymeric substances. *Environmental Science & Technology* **2016,** *50*, (11), 5498-5505.

41. Yu, Q.; Szymanowski, J.; Myneni, S. C. B.; Fein, J. B., Characterization of sulfhydryl sites within bacterial cell envelopes using selective site-blocking and potentiometric titrations. *Chem Geol* **2014,** *373*, 50-58.

42. Hu, H. Y.; Lin, H.; Zheng, W.; Rao, B.; Feng, X. B.; Liang, L. Y.; Elias, D. A.; Gu, B. H., Mercury reduction and cell-surface adsorption by geobacter sulfurreducens pca. *Environmental Science & Technology* **2013,** *47*, (19), 10922-10930.

43. Proux, O.; Lahera, E.; Del Net, W.; Kieffer, I.; Rovezzi, M.; Testemale, D.; Irar, M.; Thomas, S.; Aguilar-Tapia, A.; Bazarkina, E. F.; Prat, A.; Tella, M.; Auffan, M.; Rose, J.; Hazemann, J.-L., High-energy resolution fluorescence detected x-ray absorption spectroscopy: A powerful new structural tool in environmental biogeochemistry sciences. *Journal of Environmental Quality* **2017,** *46*, (6), 1146-1157.

44. Manceau, A.; Lemouchi, C.; Rovezzi, M.; Lanson, M.; Gatzel, P.; Nagy, K. L.; Gautier-Luneau, I.; Joly, Y.; Enescu, M., Structure, bonding, and stability of mercury complexes with thiolate and thioether ligands from high-resolution xanes spectroscopy and first-principles calculations. *Inorganic Chemistry* **2015,** *54*, (24), 11776-11791.

45. Masip, L.; Veeravalli, K.; Georgioui, G., The many faces of glutathione in bacteria. *Antioxid Redox Sign* **2006,** *8*, (5-6), 753-762.

46. Slowey, A. J., Rate of formation and dissolution of mercury sulfide nanoparticles: The dual role of natural organic matter. *Geochim Cosmochim Ac* **2010,** *74*, (16), 4693-4708.

47. Poulin, B. A.; Gerbig, C. A.; Kim, C. S.; Stegemeier, J. P.; Ryan, J. N.; Aiken, G. R., Effects of sulfide concentration and dissolved organic matter characteristics on the structure of nanocolloidal metacinnabar. *Environmental Science & Technology* **2017,** *51*, (22), 13133-13142.

48. Enescu, M.; Nagy, K. L.; Manceau, A., Nucleation of mercury sulfide by dealkylation. *Sci Rep-Uk* **2016,** *6*.

49. Enescu, M.; Manceau, A., High-level ab initio calculation of the stability of mercury-thiolate complexes. *Theor Chem Acc* **2014,** *133*, (3).

50. Manceau, A.; Wang, J.; Rovezzi, M.; Glatzel, P.; Feng, X., Biogenesis of mercury–sulfur nanoparticles in plant leaves from atmospheric gaseous mercury. *Environmental Science & Technology* **2018,** *52*, (7), 3935-3948.

51. Wright, J. G.; Tsang, H. T.; Pennerhahn, J. E.; Ohalloran, T. V., Coordination chemistry of the hg-merr metalloregulatory protein - evidence for a novel tridentate hg-cysteine receptor-site. *J Am Chem Soc* **1990,** *112*, (6), 2434-2435.

52. Parks, J. M.; Smith, J. C., Chapter five - modeling mercury in proteins. In *Methods in enzymology*, Voth, G. A., Ed. Academic Press: 2016; Vol. 578, pp 103-122.

53. Smith, S. D.; Bridou, R.; Johs, A.; Parks, J. M.; Elias, D. A.; Hurt, R. A.; Brown, S. D.; Podar, M.; Wall, J. D., Site-directed mutagenesis of hgca and hgcb reveals amino acid residues important for mercury methylation. *Applied and Environmental Microbiology* **2015,** *81*, (9), 3205-3217.

54. Zhou, J.; Riccardi, D.; Beste, A.; Smith, J. C.; Parks, J. M., Mercury methylation by hgca: Theory supports carbanion transfer to hg(ii). *Inorganic Chemistry* **2014,** *53*, (2), 772-777.

55. Qian, C.; Johs, A.; Chen, H.; Mann, B. F.; Lu, X.; Abraham, P. E.; Hettich, R. L.; Gu, B., Global proteome response to deletion of genes related to mercury methylation and dissimilatory metal reduction reveals changes in respiratory metabolism in geobacter sulfurreducens pca. *Journal of Proteome Research* **2016,** *15*, (10), 3540-3549.

56. Date, S. S.; Parks, J. M.; Rush, K. W.; Wall, J. D.; Ragsdale, S. W.; Johs, A., Kinetics of enzymatic mercury methylation at nanomolar concentrations catalyzed by hgcab. *Applied and Environmental Microbiology* **2019,** *85*, (13), e00438-19.

57. Goñi-Urriza, M.; Corsellis, Y.; Lanceleur, L.; Tessier, E.; Gury, J.; Monperrus, M.; Guyoneaud, R., Relationships between bacterial energetic metabolism, mercury methylation potential, and hgca/hgcb gene expression in desulfovibrio dechloroacetivorans beroc1. *Environmental Science and Pollution Research* **2015,** *22*, (18), 13764-13771.

58. Liu, Y. R.; Lu, X.; Zhao, L. D.; An, J.; He, J. Z.; Pierce, E. M.; Johs, A.; Gu, B. H., Effects of cellular sorption on mercury bioavailability and methylmercury production by desulfovibrio desulfuricans nd132. *Environmental Science & Technology* **2016,** *50*, (24), 13335-13341.

59. Zhao, L.; Li, Y.; Zhang, L.; Zheng, J.; Pierce, E. M.; Gu, B., Mercury adsorption on minerals and its effect on microbial methylation. *ACS Earth and Space Chemistry* **2019**.

60. Graham, A. M.; Bullock, A. L.; Maizel, A. C.; Elias, D. A.; Gilmour, C. C., Detailed assessment of the kinetics of hg-cell association, hg methylation, and methylmercury degradation in several desulfovibrio species. *Applied and Environmental Microbiology* **2012,** *78*, (20), 7337-7346.

TOC